

Article

A Shoreline Evolution Model with a Groin Structure under Non-Uniform Breaking Wave Crest Impact

Pidok Unyapoti ^{1,2,†} and Nopparat Pochai ^{1,2,*,†}

¹ Department of Mathematics, Faculty of Science, King Mongkut's Institute of Technology Ladkrabang, Bangkok 10520, Thailand; pidokunyapoti@gmail.com

² Centre of Excellence in Mathematics, CHE, Si Ayutthaya Road, Bangkok 10400, Thailand

* Correspondence: nopparat.po@kmitl.ac.th

† These authors contributed equally to this work.

Abstract: Beach erosion is a natural phenomenon that is not compensated by depositing fresh material on the shoreline while transporting sand away from the shoreline. There are three phenomena that have a serious influence on the coastal structure, such as increases in flooding, accretion, and water levels. In addition, the prediction of coastal evolution is used to investigate the topography of the beach. In this research, we present a one-dimensional mathematical model of shoreline evolution, and the parameters that influence this model are described on a monthly basis over a period of one year. Consideration is given to the wave crest impact model for evaluating the impact of the wave crest at that stage. It focuses on the evolution of the shoreline in environments where groins are installed on both sides. The initial and boundary condition setting techniques are proposed by the groins and their environmental parameters. The non-uniform influence of the crest of the breaking wave is so often considered. We then used the traditional forward time centered space technique and the Saulyev finite difference technique to estimate the monthly evolution of the shoreline for each year.

Keywords: shoreline evolution; groin system; explicit finite difference methods; wave crest impact; mathematical model



Citation: Unyapoti, P.; Pochai, N. A Shoreline Evolution Model with a Groin Structure under Non-Uniform Breaking Wave Crest Impact. *Computation* **2021**, *9*, 42. <https://doi.org/10.3390/computation9040042>

Academic Editors: Yongwimon Lenbury, Ravi P. Agarwal, Philip Broadbridge and Dongwoo Sheen

Received: 4 March 2021
Accepted: 20 March 2021
Published: 26 March 2021

Publisher's Note: MDPI stays neutral with regard to jurisdictional claims in published maps and institutional affiliations.



Copyright: © 2021 by the authors. Licensee MDPI, Basel, Switzerland. This article is an open access article distributed under the terms and conditions of the Creative Commons Attribution (CC BY) license (<https://creativecommons.org/licenses/by/4.0/>).

1. Introduction

Beach erosion is a natural process which occurs whenever the transport of material away from the shoreline is not balanced by new material being deposited onto the shoreline. This is a problem that causes a decrease in beach areas. In order to prevent beach erosion and beach deposition which may devise a sea wall and groin, in [1], the design of the functional groin and a simulation of the action of single and multiple groins using GENESIS was proposed. Predictions of shoreline changes have been tested at 15 groins in Westhampton, Long Island, and New York. In [2], changes in the beach profile due to the construction of a single zigzag type of porous groin, named GROPOZAG, were reported.

Qualitative awareness of the idealized reaction of the shoreline to the governance process is required to examine beach erosion and beach deposition. The only instrument which can consider this is an analytical solution based on a mathematical model that explains fundamental physics. Many authors have developed an analytical solution to the evolution of the shoreline using a basic mathematical formula. Many authors have developed a one-line theory, and several contributors have included [3–8] in the analytical solution of the evolution of the shoreline. It cannot be assumed that the analytical solution would have quantitatively precise solutions to the problems containing complex boundary conditions and wave inputs. In the actual case, a numerical model of the evolution of the shoreline will be more fitting. In [9,10], the authors used conditionally stable explicit finite difference methods to approximate their model solutions.

In [11], the authors proposed a numerical model developed for the site conditions, which was used to measure the impact of lengthening the groin to a depth of 5 m to position it across the zone of bar migration. The model accurately represents observed processes, predicting less scour and more deposition at the coastal tip of the extended groin, as well as an increased probability of a rip current near the structure at Marina di Ronchi, Italy. In [12], a new numerical scheme for simulating flows around buildings with sharp-cornered structures was proposed. The proposed numerical model was tested against a well-known present experiment involving a wave group entering a shoreline and the presence of a T-head groin design. In [13], the effect of a groin application to erosion at the shoreline was proposed. The method utilized the bathymetry and topography data of the north beach of Balongan, West Java. In [14], probabilistic changes to the shoreline were calculated by using two simulations. The first simulation was the GenCade simulation, which was used to predict the long-term evolution of the shoreline induced by natural offshore waves. The second was the Monte Carlo simulation, which was used to simulate the evolution of the shoreline in response to changes in sea level. In [15], the ONELINE modeling method was presented, and its capabilities were demonstrated by model testing of two case studies. The first one has a groin area at Sea Isle City, New Jersey along the East Coast of the United States. The second is along the Nile Delta Coast in Egypt. In [16], a comparison between the analytic and numerical solutions in the idealized wave condition for four different shoreline configurations was proposed.

In this research, we introduce a governing equation of a one-dimensional shoreline evolution model when a couple of groins is added. We introduce a non-uniform impact effect of the breaking wave crest. We introduce the initial condition and the boundary conditions setting. Finite difference techniques will be used to approximate the model solution. A numerical model is being developed to predict the efficiency of the groin effect on shoreline evolution. We focus on predicting the efficiency of a straight, impermeable groin.

2. Governing Equation

2.1. Shoreline Evolution Model

In a one-dimensional shoreline evolution model, while maintaining the same shape, the beach shape is supposed to move towards land and towards the sea, meaning that all the bottom outlines become parallel. As a result, under this presumption, it is necessary to define the horizontal position of the shape relative to the baseline, and one outline could be used to explain changes in the form and volume of the beach plane as the beach erodes and accretes. The model's main assumption is that the sand is transported alongshore on the profile between two well-defined limiting elevations. If there is a disparity in the long-shore sand transport rate on the side of the segment and the related s and consistency, one contribution would be to obtain volume adjustment results. The principles of conservation of mass must be applied to the system at all times. The corresponding differential equation for the evolution of the shoreline is generated by considering the definitions above.

$$\frac{\partial y}{\partial t} = \frac{1}{D_B + D_C} \left(-\frac{\partial Q}{\partial x} \right), \quad (1)$$

where x is the co-ordinate on the shores (m), y is the location of the shoreline (m) and is perpendicular to the x -axis, t is time (day), Q is the long-shore sand transport rate (m^3/day), D_B is the average height of the berm (m), and D_C is the average depth of closure (m). To solve Equation (1), it was necessary to define a term for the long-shore sand transport rate (Q). This quantity is assumed to have been obtained by the oblique wave occurring at the shoreline. The US Army Corp developed a generalized term for the long-shore sand transport rate [17]:

$$Q = Q_0 \sin(2\alpha_b), \quad (2)$$

where Q_0 is the long-shore sand transport rate amplitude, and α_b is the angle between the breaking wave crest impact angle and local shoreline. The general formula for the long-shore sand transport rate amplitude is as follows [18]:

$$Q_0 = \frac{\rho}{16} (H_b^2 c_{gb}) \frac{K}{(\rho_s - \rho)(1 - n)}, \tag{3}$$

where the b subscription signifies the value at the breaking point, c_g is the velocity of the wave group, H is the wave height, ρ_s is the sediment density (kg/m^3), ρ is the sea water's density, n is the porosity, and K is the non-dimensional coefficient of the particle size function, and α_b can be written as:

$$\alpha_b = \alpha_0 - \tan^{-1} \left(\frac{\partial y}{\partial x} \right), \tag{4}$$

where α_0 is the angle between breaking wave crests' impact angle and x-axis. It can be assumed for beaches with a mild slope that the angle of the wave breaking to the shoreline is minimal. Assuming that

$$\sin(2\alpha_b) \approx 2\alpha_b, \tag{5}$$

and

$$\tan^{-1} \left(\frac{\partial y}{\partial x} \right) \approx \frac{\partial y}{\partial x}, \tag{6}$$

replacing the Equation (2) with the Equation (4), and assuming that the beach has a mild slope:

$$Q = Q_0 \left(2\alpha_b - 2 \frac{\partial y}{\partial x} \right), \tag{7}$$

replacing the Equation (1) with the Equation (7) and ignoring the sources or sinks along the shoreline provides the following:

$$\frac{\partial y}{\partial x} = D \frac{\partial^2 y}{\partial x^2}, \tag{8}$$

for all $(x, t) \in (L, T)$, where

$$D = \frac{2Q_0}{D_B + D_C}. \tag{9}$$

Equation (8) is similar to a one-dimensional heat diffusion equation, which can be solved analytically under varying initial and boundary conditions.

2.2. Physical Parameters

The physical parameter of the model can be illustrated as shown in Figures 1 and 2 that are listed below.

- α_0 is the angle between breaking wave crests' impact angle and x-axis.
- Q_0 is the long-shore sand transport rate amplitude.
- D_B is the average height of the berm.
- D_C is the average depth of closure.
- L is alongshore.
- T is the time of simulation.

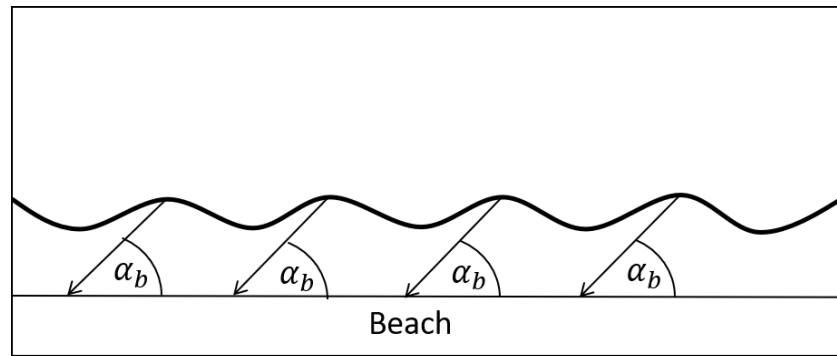


Figure 1. Breaking wave crests' impact angle.

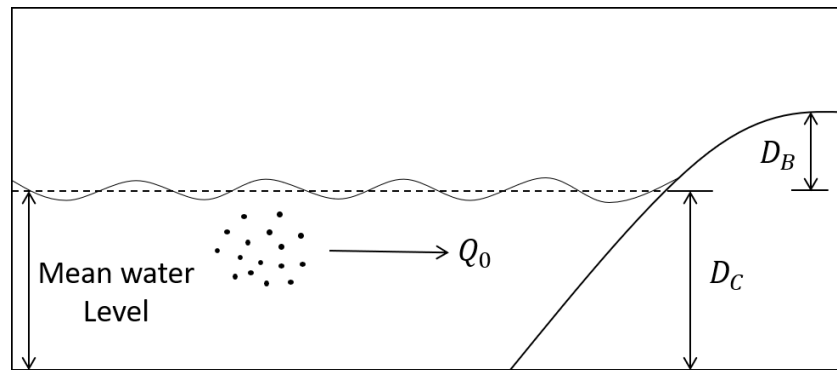


Figure 2. Shoreline's physical parameters.

2.3. The Initial and Boundary Conditions

Straight, impermeable groin system. The initial shoreline is assumed to be parallel to the x-axis. Assuming that, the sand transport rate along the shoreline is uniform. The groin is instantaneously added at $x = 0$, as shown in Figure 3. This means that the initial condition becomes,

$$y(x, 0) = 0, \tag{10}$$

the wave crest impact effect to the boundary condition setting. This means that the boundary condition becomes,

$$\frac{\partial y(0, t)}{\partial x} = -\tan(\alpha_0) \text{ at } x = 0, \tag{11}$$

and

$$\frac{\partial y(L, t)}{\partial x} = -\tan(-\alpha_0) \text{ at } x = L. \tag{12}$$

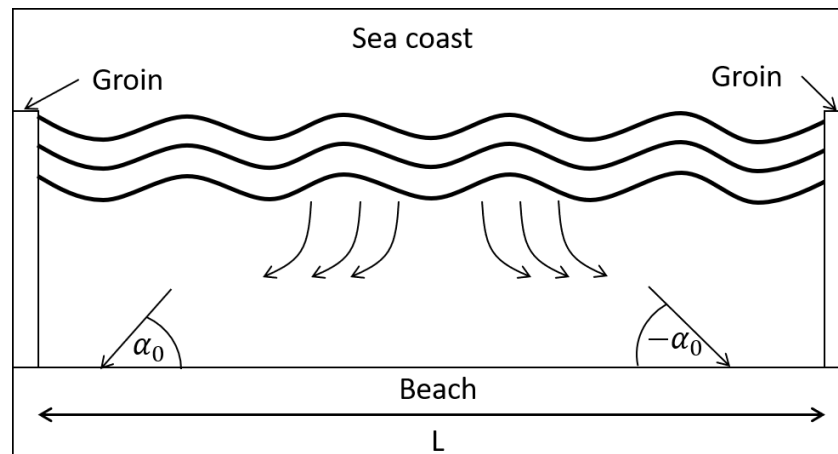


Figure 3. Initial shoreline.

2.4. Wave Crest Impact Model

The hydrodynamic model is introduced to obtain the wave crest impact in the shoreline evolution model [19].

The two-dimensional unstable water flow into and out of the seashore may be calculated by the use of a system of shallow water equations, taking into consideration the mass conservation and the momentum conservation. The equations of this method should be derived from the vertical direction of the depth-averaging of the Navier-Stokes equations, neglecting the diffusion of momentum due to vibration and discarding the terms representing the effects of friction, surface wind, Coriolis factor, and shear stress. The equation of continuity is then expressed as follows:

$$\frac{\partial h}{\partial t} + \frac{\partial(uh)}{\partial x} + \frac{\partial(vh)}{\partial y} = 0, \tag{13}$$

and the momentum equations are expressed as below:

$$\frac{\partial(uh)}{\partial t} + \frac{\partial\left(u^2h + \frac{1}{2}gh^2\right)}{\partial x} + \frac{\partial(uvh)}{\partial y} = 0, \tag{14}$$

$$\frac{\partial(vh)}{\partial t} + \frac{\partial(uvh)}{\partial x} + \frac{\partial\left(v^2h + \frac{1}{2}gh^2\right)}{\partial y} = 0, \tag{15}$$

where

- $h(x, y, t)$ is the depth estimated from the average water surface to the seashore bed
- $h = H + \zeta(\mathbf{m})$,
- $\zeta(x, y, t)$ is the elevation of water surface from the average water level at seashore (m),
- $H(x, y)$ is the interpolated bottom topography function of the seashore (m),
- $u(x, y, t)$ is velocity in the direction of x (m/s),
- $v(x, y, t)$ is velocity in the direction of y (m/s),
- g is a constant in gravity (9.8 m/s²).

Such time (t), and two space coordinates, x and y are the independent variables. Likewise, the conserved quantities are mass, which is proportional to h , and momentum, which is proportional to (uh) and (vh) . As taken with respect to the same term, the partial

derivatives are grouped into vectors $(\partial x, \partial y, \partial t)$ and then rewritten as a partial differential hyperbolic equation, as follows:

$$U = \begin{pmatrix} h \\ uh \\ vh \end{pmatrix}, F(U) = \begin{pmatrix} uh \\ u^2h + \frac{1}{2}gh^2 \\ uvh \end{pmatrix}, G(U) = \begin{pmatrix} vh \\ uvh \\ v^2h + \frac{1}{2}gh^2 \end{pmatrix}. \tag{16}$$

The hyperbolic PDE:

$$\frac{\partial U}{\partial t} + \frac{\partial F(U)}{\partial x} + \frac{\partial G(U)}{\partial y} = 0. \tag{17}$$

2.5. The Initial and Boundary Condition for Wave Crest Impact Model

The initial conditions of the reservoir were as follows: The x - and y -velocity components were zero, as well as the water elevation of $u = 0, v = 0$, and $\zeta = 0$.

Assuming that the break-water is not a perfect barrier to water as it is made of an aggregate of rocks with large gaps, the boundary conditions were as follows: (i) $u = 0, \frac{\partial v}{\partial y} = 0, \zeta = f(x, y, t)$ for waves coming into the beach, (ii) $\frac{\partial u}{\partial x} = 0, v = 0, \frac{\partial \zeta}{\partial x} = 0$ for left and right groin structures, and (iii) $u = 0, \frac{\partial v}{\partial y} = 0, \frac{\partial \zeta}{\partial y} = 0$ for along the beach, as shown in Figure 4.

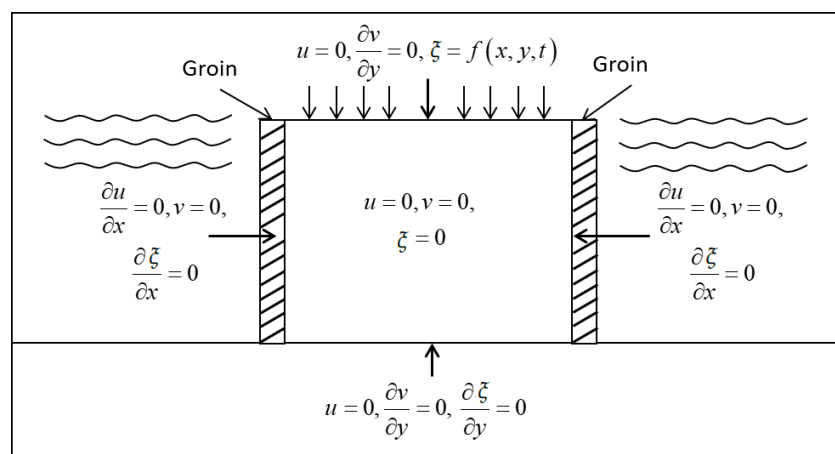


Figure 4. Initial and boundary conditions.

3. Numerical Techniques

3.1. Grid Spacing

We now discretize Equation (8) by dividing the interval $[0, L]$ into M sub-intervals, such that $M\Delta x = L$, and the interval $[0, T]$ into N sub-intervals, such that $N\Delta t = T$. We then approximate $y(x_n, t_n)$ by y_i^n , at the point $x_i = i\Delta x$ and $t_n = n\Delta t$, where $0 \leq i \leq M$ and $0 \leq n \leq N$ in which there are positive integers of M and N .

3.2. Traditional Forward Time-Centered Space Technique

The forward time-centered space schemes is employed. Consequently, the finite difference approximation becomes [20]

$$y \cong y_i^n, \tag{18}$$

$$\frac{\partial y}{\partial t} \cong \frac{y_i^{n+1} - y_i^n}{\Delta t}, \tag{19}$$

$$\frac{\partial y}{\partial x} \cong \frac{y_{i+1}^n - y_{i-1}^n}{2\Delta x}, \tag{20}$$

$$\frac{\partial^2 y}{\partial x^2} \cong \frac{y_{i+1}^n - 2y_i^n + y_{i-1}^n}{(\Delta x)^2}, \tag{21}$$

where $A = \frac{D\Delta t}{(\Delta x)^2}$.

Replacing the Equation (8) with the Equations (18)–(21), we obtain

$$\frac{y_i^{n+1} - y_i^n}{\Delta t} = D \left(\frac{y_{i+1}^n - 2y_i^n + y_{i-1}^n}{(\Delta x)^2} \right), \tag{22}$$

for $1 \leq i \leq M - 1$ and $0 \leq n \leq N - 1$. Equation (22) can be written in an explicit form of finite difference as follows,

$$y_i^{n+1} = Ay_{i+1}^n + (1 - 2A)y_i^n + Ay_{i-1}^n, \tag{23}$$

for $1 \leq i \leq M - 1$ and $0 \leq n \leq N - 1$.

3.3. Unconditionally Saulyev Finite Difference Techniques

The Saulyev scheme is employed. Consequently, the finite difference approximation becomes [9]

$$y \cong y_i^n, \tag{24}$$

$$\frac{\partial y}{\partial t} \cong \frac{y_i^{n+1} - y_i^n}{\Delta t}, \tag{25}$$

$$\frac{\partial^2 y}{\partial x^2} \cong \frac{y_{i+1}^n - y_i^n - y_i^{n+1} + y_{i-1}^{n+1}}{(\Delta x)^2}, \tag{26}$$

where $A = \frac{D\Delta t}{(\Delta x)^2}$.

Replacing the Equation (8) with the Equations (24)–(26), we obtain

$$\frac{y_i^{n+1} - y_i^n}{\Delta t} = D \left(\frac{y_{i+1}^n - y_i^n - y_i^{n+1} + y_{i-1}^{n+1}}{(\Delta x)^2} \right), \tag{27}$$

for $1 \leq i \leq M - 1$ and $0 \leq n \leq N - 1$. Equation (27) can be written in an explicit form of finite difference as follows,

$$y_i^{n+1} = \frac{1}{1 + A} (Ay_{i+1}^n + (1 - A)y_i^n + Ay_{i-1}^{n+1}), \tag{28}$$

for $1 \leq i \leq M - 1$ and $0 \leq n \leq N - 1$.

3.4. Numerical Techniques for the Wave Crest Impact Model

The finite difference technique [19]:

$$U_{i,j}^{n+1} = U_{i,j}^n - \frac{\Delta t}{\Delta x} \left(F_{i+\frac{1}{2},j}^{n+\frac{1}{2}} - F_{i-\frac{1}{2},j}^{n+\frac{1}{2}} \right) - \frac{\Delta t}{\Delta y} \left(G_{i,j+\frac{1}{2}}^{n+\frac{1}{2}} - G_{i,j-\frac{1}{2}}^{n+\frac{1}{2}} \right). \tag{29}$$

3.5. The Wave Crest Impact

The wave crest impact becomes

$$\alpha(x_i, y_j, t) = \tan^{-1} \left(\frac{v(x_i, y_j, t)}{u(x_i, y_j, t)} \right), \tag{30}$$

and the averaged wave crest impact is assumed by

$$\alpha_0(t) = \frac{\sum_{i=1}^{N_p} \alpha(x_i, 0, t)}{N_p}, \tag{31}$$

where N_p is a number of wave crest impact sample points along the shoreline.

3.6. The Employment of Traditional Forward Time-Centered Space Technique to the Left and the Right Boundary Conditions

The forward time-centered space method is employed. Consequently, the finite difference approximation becomes

$$y \cong y_i^n, \tag{32}$$

$$\frac{\partial y}{\partial t} \cong \frac{y_i^{n+1} - y_i^n}{\Delta t}, \tag{33}$$

$$\frac{\partial y}{\partial x} \cong \frac{y_{i+1}^n - y_{i-1}^n}{2\Delta x}, \tag{34}$$

$$\frac{\partial^2 y}{\partial x^2} \cong \frac{y_{i+1}^n - 2y_i^n + y_{i-1}^n}{(\Delta x)^2}, \tag{35}$$

where $A = \frac{D\Delta t}{(\Delta x)^2}$.

Replacing the Equation (8) with the Equations (32)–(35), we obtain

$$\frac{y_i^{n+1} - y_i^n}{\Delta t} = D \left(\frac{y_{i+1}^n - 2y_i^n + y_{i-1}^n}{(\Delta x)^2} \right), \tag{36}$$

for $i = 0$, where replacing the uncertain value of the left boundary is approximated by the method of center difference with the specified left boundary condition

$$y_{-1}^n = y_1^n - 2(\Delta x)(-\tan(\alpha_0)), \tag{37}$$

replacing the Equation (36) with the Equation (37), we obtain

$$y_i^{n+1} = (1 - 2A)y_i^n + 2Ay_{i+1}^n - 2A(\Delta x)(-\tan(\alpha_0)), \tag{38}$$

for $i = M$, replacing the uncertain value of the right boundary is approximated by the method of center difference with the specified right boundary condition

$$y_{M+1}^n = y_{M-1}^n + 2(\Delta x)(-\tan(-\alpha_0)), \tag{39}$$

replacing the Equation (36) with the Equation (39), we obtain

$$y_i^{n+1} = 2Ay_{i-1}^n + (1 - 2A)y_i^n + 2A(\Delta x)(-\tan(-\alpha_0)). \tag{40}$$

The Equations (38) and (40) could be used to approximate the y_i^n values on the solution’s domain grid points.

4. Physical Parameters’ Setting Techniques

Assuming that the sediment density (ρ_s) [21], the sea water’s density (ρ) [22], the porosity (n) [23], the non-dimensional coefficient of the particle size function (K) [24], the average height of the berm (D_B), and the average depth of closure (D_C) are listed below.

The wave group velocity (c_g) and the wave height (H) in each month along a year measured by field data on the gulf of Thailand are collected by the GeoInformatics and Space Technology Development Agency (Public Organization) (GISTDA) [25], as listed below.

The long-shore sand transport rate amplitude (Q_0) is obtained by Equation (3) and the long-shore transport rates (D) are obtained by Equation (9), as listed below.

5. Numerical Experiment

To analyze the evolution of the shoreline on a long-term scale, the numerical results of the beach scenario are considered and the solution to the idealized problem is introduced.

Assuming, during the simulation, that the length of the shoreline considered is $L = 100$ m, we set the physical parameter in Tables 1–3. The simulation setting is illustrated in Figure 3.

We will employ the finite difference techniques Equation (29) to approximate the wave crest impact model solution, as shown in Figure 5.

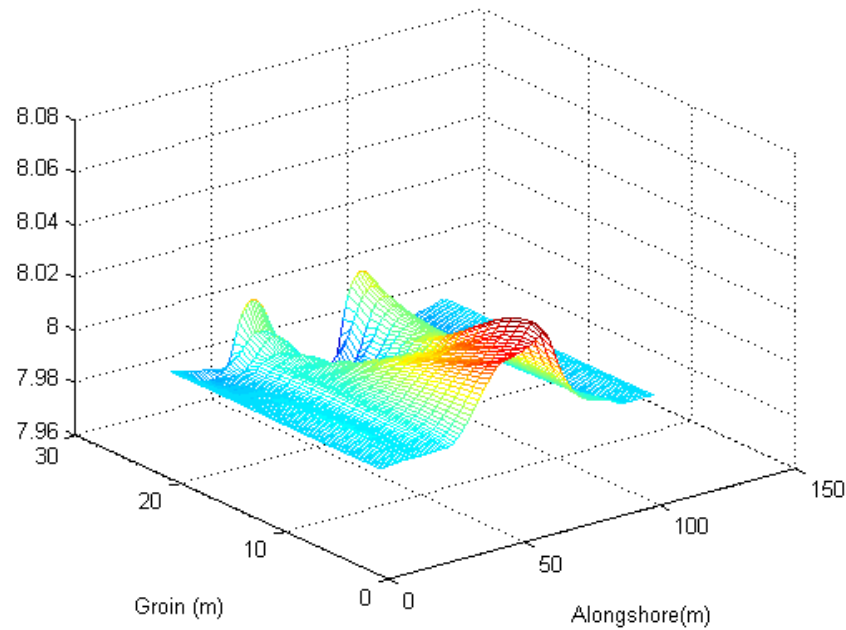


Figure 5. Wave crest impact in one year (360 days).

Table 1. Parameters of sand transport rate.

The sediment density (ρ_s (kg/m ³))	1700
The sea water's density (ρ (kg/m ³))	1020
The porosity (n)	0.406
The non-dimensional coefficient of the particle size function (K)	0.375
The average height of the berm. (D_B (m))	2
The average depth of closure. (D_C (m))	8

Table 2. The wave group velocity and the wave height.

Month	c_g (m/day)	H (m)
January 2019	8951.04	1.5
February 2019	6998.4	1.5
March 2019	5866.56	0.5
April 2019	6920.64	1.5
May 2019	5719.68	0.5
June 2019	5546.88	0.5
July 2018	8225.28	1.5
August 2018	9357.12	1.5
September 2018	13,711.68	1.5
October 2018	15,085.44	2.5
November 2018	10,877.76	1.5
December 2018	11,396.16	1.5

Table 3. The amplitude of the longshore transport rates and the longshore transport rates.

Month	Q_0 (m/day)	D (m/day)
January 2019	1191.99	238.3977
February 2019	931.96	186.3921
March 2019	86.80	17.3607
April 2019	921.61	184.3209
May 2019	84.63	16.9260
June 2019	82.07	16.4148
July 2018	1095.34	219.0681
August 2018	1246.07	249.2130
September 2018	1825.95	365.1903
October 2018	5580.26	1116.0520
November 2018	1448.57	289.7130
December 2018	1517.60	303.3699

The averaged wave crest impact (α_0) is obtained by Equation (31), as shown in Table 4.

Table 4. The averaged wave crest impact in one year (360 days).

Time	min						
day	0–90	90–180	180–270	270–360	360–450	450–540	540–630
30	−0.0186	−0.0185	−0.0184	−0.0182	−0.0181	−0.0180	−0.0179
60	0.0052	0.0052	0.0051	0.0051	0.0051	0.0051	0.0050
90	0.0623	0.0621	0.0619	0.0617	0.0615	0.0614	0.0612
.
.
360	0.1306	0.1306	0.1306	0.1306	0.1306	0.1306	0.1306

Time	min						
day	630–720	720–810	810–900	900–990	990–1080	1080–1170	1170–1260
30	−0.0178	−0.0178	−0.0177	−0.0176	−0.0175	−0.0175	−0.0174
60	0.0049	0.0048	0.0047	0.0046	0.0046	0.0046	0.0046
90	0.0610	0.0608	0.0606	0.0604	0.0602	0.0600	0.0598
.
.
360	0.1307	0.1618	0.1618	0.1618	0.1618	0.1618	0.1619

Time	min	
day	1260–1350	1350–1440
30	−0.0173	−0.0172
60	0.0046	0.0046
90	0.0597	0.0595
.	.	.
.	.	.
360	0.1619	0.1619

We will employ the traditional forward time-centered space technique (23), and the Saulyev finite difference techniques (28), to approximate the model solution. The calculated results $L = 100$ m are as shown in Figure 6.

The approximated solutions of the traditional forward time-centered space technique and Saulyev finite difference techniques give approximated solutions in Tables 5 and 6.

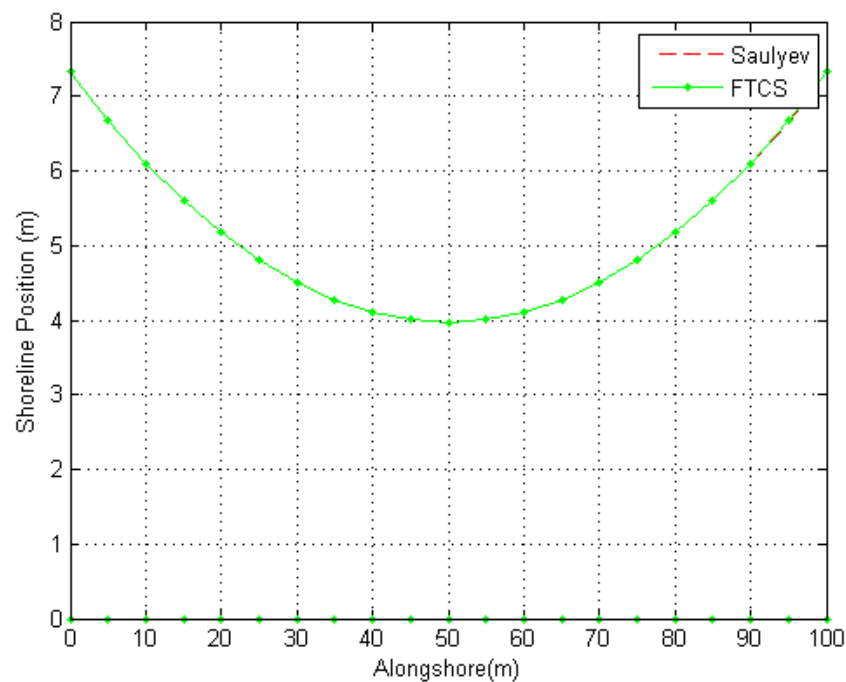


Figure 6. Shoreline evolution in one year.

Table 5. Approximated shoreline evolution along one year by a traditional forward time-centered space technique.

Time (years)	Distance (m)					
	0	20	40	60	80	100
1	7.3252	5.1761	4.1060	4.1060	5.1761	7.3252

Table 6. Approximated shoreline evolution along one year by Saulyeve finite difference techniques.

Time (years)	Distance (m)					
	0	20	40	60	80	100
1	7.3260	5.1764	4.1053	4.1060	5.1756	7.3238

6. Discussion

The effect of the wave crest from Equation (31) as shown in Table 4. The long-shore transport rates (D) are also measured on a monthly basis during the year. The long-shore transport rates (D) were obtained by using Equation (9). The amplitude of the long-shore transport rates (Q_0) was obtained by Equation (3), the density of the sediment (ρ_s), the density of seawater (ρ), the porosity (n), the non-dimensional coefficient of the particle size function (K), the averaged berm height (D_B) and the closure depth (D_C), as shown in Table 1. The wave group velocity (c_g) and the wave height (H) for each month are seen in Table 2. The amplitude of the long-distance transport rate (Q_0) and the long-distance transport rate (D) for each month are simulated as shown in Table 3.

The evolution of the coastline in each year is predicted by the use of a traditional forward time-centered space technique and Saulyeve finite difference techniques, as seen in Tables 5 and 6 and Figure 3. The distance from the most distant shoreline evolution is 7.32 m. The shortest distance from the shoreline evolution is 3.96 m. The calculated shoreline evolution of the two numerical techniques is closed.

7. Conclusions

In this research, we presented a one-dimensional mathematical model of shoreline evolution, and the parameters that affect this model are presented monthly over one year. The wave crest impact model was used to estimate the nonuniform breaking wave crest impact at the time it was considered. The evolution of the shoreline in areas where groins are installed on both sides was focused on. The initial and boundary conditions were defined by the groins on both sides. We then used the traditional forward time-centered space technique and Saul'yev finite difference techniques to estimate the monthly evolution of the shoreline for each year. The traditional forward time-centered space technique provides a more accurate measurement than the Saul'yev finite difference techniques. However, if any time increment cases are chosen, the traditional forward time-centered space technique is not capable of estimating the solution—see also [26]. Fortunately, the solution can always be estimated by the Saul'yev finite difference techniques. The approximate effects of the shoreline evolution were consistent with the nonuniform breaking wave crest impact by the wave crest impact model and the installation properties of the beach groins.

Author Contributions: Conceptualization, N.P.; investigation, N.P. and P.U.; project administration, N.P.; supervision, N.P.; writing—original draft, N.P. and P.U.; writing—review and editing, N.P. All authors have read and agreed to the published version of the manuscript.

Funding: The Centre of Excellence in Mathematics, the Commission on Higher Education, Thailand.

Institutional Review Board Statement: Not applicable.

Informed Consent Statement: Not applicable.

Data Availability Statement: All data generated or analysed during this study are included in this published article.

Acknowledgments: This paper is supported by the Centre of Excellence in Mathematics, the Commission on Higher Education, Thailand.

Conflicts of Interest: The authors declare no conflict of interest.

References

1. Hanson, H.; Kraus, N.C.; Blomgren, S.H. Modern functional design of groin systems. *Coast. Eng.* **1994**, *96*, 1327–1342.
2. Fatimah, E.; Ariff, A.; Aulia, T.B. The influence of single zigzag type porous groin in the change of beach profile. *Procedia Eng.* **2015**, *125*, 257–262. [CrossRef]
3. Bakker, W.T.; Breteler, E.K.; Roos, A. The dynamics of coast with a groin system. *Coast. Eng. Proc.* **1970**, *1*, 492–517. doi:10.9753/icce.v12.64. [CrossRef]
4. Bakker, W.T.; Edelman, T. The coastline of river deltas. *Coast. Eng. Proc.* **1964**, *1*, 199–218. doi:10.9753/icce.v9.13. [CrossRef]
5. Grijm, W. Theoretical form of shoreline. Available online: <https://ascelibrary.org/doi/abs/10.1061/9780872620056.014> (accessed on 25 March 2021).
6. Mahute, B.L.; Soldate, M. Mathematical Modeling of Shoreline Evolution. In *US Army Corps of Engineer Waterways Experiment Station*; CERC: Rockville, MD, USA, 1977.
7. Hanson, H.; Larson, M.; Kraus, N.C. Analytical Solution of the One-line Model for Shoreline Change. In *US Army Corps of Engineer Waterways Experiment Station*; CERC: Rockville, MD, USA, 1987.
8. Walton, T.; Chiu, T. A review of analytical technique to solve the sand transport equation and some simplified solution. *Coast. Struct.* **1979**, 809–837.
9. Pochai, P. Unconditional stable numerical techniques for a water-quality model in a non-uniform flow stream. *Adv. Differ. Eq.* **2017**, *2017*, 13. [CrossRef]
10. Samalerk, P.; Pochai, N. Numerical Simulation of a One-Dimensional Water-Quality Model in a Stream Using a Saul'yev Technique with Quadratic Interpolated Initial-Boundary Conditions. *Abstr. Appl. Anal.* **2018**, *2018*, 1926519. [CrossRef]
11. Aminti, P.; Cammelli, C.; Cappietti, L.; Jackson, N.L.; Nordstrom, K.F.; Pranzini, E. Evaluation of Beach Response to Submerged Groin Construction at Marina di Ronchi, Italy, Using Field Data and a Numerical Simulation Model. *J. Coast. Res.* **2004**, *33*, 99–120.
12. Cannata, G.; Tamburrino, M.; Gallerano, F. 3D Numerical Simulation of the Interaction between Waves and a T-Head Groin Structure. *J. Mar. Sci. Eng.* **2020**, *8*, 227. [CrossRef]
13. Setyandito, O.; Purnama, A.C.; Yuwono, N.J.; Wijayanti, Y. Shoreline Change with Groin Coastal Protection Structure at North Java Beach. *ComTech Comput. Math. Eng. Appl.* **2020**, *11*, 19–28. [CrossRef]

14. Ding, Y.; Kim, S.; Frey, A.E. Probabilistic Shoreline Evolution Modeling in Response to Sea Level Changes. *World Environ. Water Resour. Congr.* **2018**. [[CrossRef](#)]
15. Dabees, M.; Kamphuis, J.W. Oneline, A Numerical Model for Shoreline Change. In *Proceeding of the 26th Coastal Engineering Conference 1998, Copenhagen, Denmark, 22–26 June 1998*; pp. 2668–2681.
16. Subiyanto, M.M.; Ahmad, M.F.; Husain, M.L. Comparison of numerical method for forward and backward time centered space for long—Term simulation of shoreline evolution. *Appl. Math. Sci.* **2013**, *7*, 5165–5173. [[CrossRef](#)]
17. US Army Corp of Engineers. *Shore Protection Manual*; Coastal Engineering Research Centre: Washington, DC, USA, 1984.
18. Hoan, L.X. Some result of comparison between numerical and analytical solutions of the one-line model for shoreline change. *Vietnam. J. Mech.* **2006**, *28*, 94–102. [[CrossRef](#)]
19. Kraychang, W.; Pochai, N. Numerical Treatment to a Water-Quality Measurement Model in an Opened-Closed Reservoir. *Thai J. Math.* **2015**, *13*, 775–788.
20. Mitchell, A.R. *Computational Methods in Partial Differential Equations*; John Wiley & Sons Ltd.: London, UK, 1969.
21. Tenzer, R.; Gladkikh, V. Assessment of density variations of marine sediments with ocean and sediment depths. *Sci. World J.* **2014**, *2014*, 823296. [[CrossRef](#)] [[PubMed](#)]
22. Wikipedia. Available online: <https://en.wikipedia.org/wiki/Seawater> (accessed on 25 March 2021).
23. Román-Sierra, J.; Muñoz-Perez, J.J.; Navarro-Pons, M. Beach nourishment effects on sand porosity variability. *Coast. Eng.* **2014**, *83*, 221–232. [[CrossRef](#)]
24. Dronkers, J.; van den Berg, J. Available online: http://www.coastalwiki.org/wiki/Coastal_and_marine_sediments?fbclid=IwAR2UkENgXUxyEJlj5tlaau2yPrDOCuRniHu3FqSCrLwVD_KpKmtqXob1iZc (accessed on 25 March 2021).
25. GeoInformatics and Space Technology Development Agency (Public Organization) (GISTDA). Available online: <http://http://coastalradar.gistda.or.th/wp/?page=announce-small> (accessed on 25 March 2021).
26. Unyapoti, P.; Pochai, N. A One-Dimensional Mathematical Model of Long-Term Shoreline Evolution with Groin System using an Unconditionally Stable Explicit Finite Difference Method. *Int. J. Simul. Syst. Sci. Technol.* **2020**, *21*, 2.1–2.6. [[CrossRef](#)]